Organometallics 1992, *11*, 2543–2550

Preparation and Crystal Structures of *syn*-$[(\mu\text{-SPh})Fe(CO)_3]_2$, $(C_5H_4SPh)_2Fe$, $(C_5H_5)Fe(C_5H_4SPh)$, and $(C_5H_4SPh)Fe(C_5H_4PPh_2)$

J. Adebanjo Adeleke,[†,‡] Yu-Wang Chen,[†,§] and Ling-Kang Liu*,[†,§]

Institute of Chemistry, Academia Sinica, Taipei 11529, Taiwan, Republic of China,
and Department of Chemistry, National Taiwan University, Taipei 10764, Taiwan, Republic of China

Received August 9, 1991

The reaction of $(C_5H_4SPh)_2Fe$ with $Fe_2(CO)_9$ in MeCN at 25 °C under photolytic conditions has been found to afford a dimer, $[(\mu\text{-SPh})Fe(CO)_3]_2$, whose X-ray structure exhibits a syn form. This reaction also yields $(C_5H_5)Fe(C_5H_4SPh)$ as a byproduct, following the C–S bond cleavage. Stepwise functionalized of $(C_5H_5)_2Fe$ *via* selective transmetalation of $(C_5H_4SnBu_3)_2Fe$ has led to the successful preparation of $(C_5H_5)Fe(C_5H_4SPh)$ and $(C_5H_4SPh)Fe(C_5H_4PPh_2)$ in good yields. X-ray crystallographic studies of the title compounds have been carried out. $(C_5H_4SPh)_2Fe$ (**2**): monoclinic space group $P2_1/c$, $a = 6.099$ (3) Å, $b = 7.855$ (1) Å, $c = 19.027$ (3) Å, $\beta = 99.12$ (2)°, $V = 902.2$ Å^3, $Z = 2$, 1976 data with $I_0 > 2.5\sigma(I_0)$ refined to $R = 0.029$ and $R_w = 0.035$. $(C_5H_5)Fe(C_5H_4SPh)$ (**3**): orthorhombic space group $P2_12_12_1$, $a = 7.307$ (8) Å, $b = 9.018$ (9) Å,$c = 20.033$ (3) Å, $V = 1320.1$ Å^3, $Z = 4$, 1054 data with $I_0 > 2.5\sigma(I_0)$ refined to $R = 0.026$ and $R_w = 0.028$. $(C_5H_4SPh)Fe(C_5H_4PPh_2)$ (**7**): triclinic space group $P\bar{1}$, $a = 9.675$ (2) Å, $b = 10.903$ (3) Å, $c = 12.899$ (3) Å, $\alpha = 112.89$ (3)°, $\beta = 86.89$ (2)°, $\gamma = 113.53$ (2)°, $V = 1141$ Å^3, $Z = 2$, 2567 data with $I_0 > 2.5\sigma(I_0)$ refined to $R = 0.032$ and $R_w = 0.040$. *syn*-$[(\mu\text{-SPh})Fe(CO)_3]_2$ (**8**): orthorhombic space group *Pbca*, $a = 7.151$ (2) Å, $b = 20.847$ (3) Å, $c = 27.155$ (4) Å, $V = 4048.0$ Å^3, $Z = 8$, 1247 data with $I_0 > 2.5\sigma(I_0)$ refined to $R = 0.043$ and $R_w = 0.043$.

Introduction

The chemistry of $(C_5H_4PPH_2)_2Fe$, dppf, upon its complexation with transition metals has attracted much interest for use in homogeneous catalysis[1] and as a possible antitumor agent.[2] As a neighboring atom to P, S usually displays different chemistry from that of P due to a larger electronegativity and a smaller atomic size for S. Brubaker reported the preparation and reactivity of a series of ferrocenyl sulfide derivatives as bidentate chelating ligands.[3] No chelation to Fe(0) for any ferrocenyl sulfide has been reported in the literature despite the fact that chelation to many other transition metals is known.[4] On the other hand, dppf chelation of Fe(0) has been characterized by spectroscopic methods as well as X-ray structure analysis.[5] It should be very interesting to see to what extent ferrocenyl sulfide derivatives react with iron carbonyls. This paper reports the isolation and structural characterization of *syn*-$[(\mu\text{-SPh})Fe(CO)_3]_2$ from a photolytic reaction of $(C_5H_4SPh)_2Fe$ with $Fe_2(CO)_9$. The anti isomer has been known in the literature for many years.[6] Nonetheless, the syn isomer is isolated and structurally characterized for the first time.

In this report the synthesis and characterization of $(C_5H_4SPh)Fe(C_5H_4PPh_2)$ is also included as the first example of a ferrocenyl ligand having both S and P donor atoms. Details of structure analysis are presented for three related ferrocenyl ligands: $(C_5H_4SPh)_2Fe$, $(C_5H_5)Fe(C_5H_4SPh)$, and $(C_5H_4SPh)Fe(C_5H_4PPh_2)$.

Scheme I

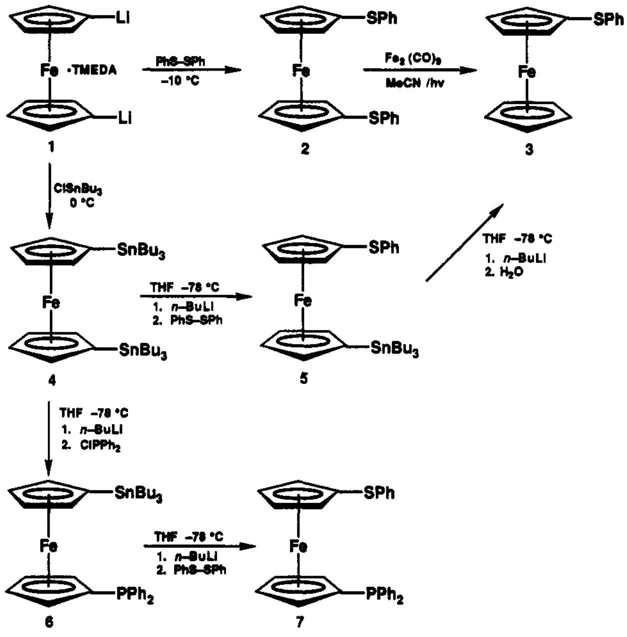

Results and Discussion

Synthesis and Characterization. The title compounds are prepared in moderate to high yields according to the reaction sequence in Scheme I. The reaction of $(C_5H_4SPh)_2Fe$ (**2**) with $Fe_2(CO)_9$ in MeCN under photolytic conditions at 25 °C has been found to afford a dimer, $[(\mu\text{-SPh})Fe(CO)_3]_2$ (**8**), whose X-ray structure exhibits a syn form (Figure 1).

$$\underset{\mathbf{1}}{(C_5H_4SPh)_2Fe} \xrightarrow[\text{MeCN}/h\nu]{Fe_2(CO)_2} \underset{\mathbf{8}}{[(\mu\text{-SPh})Fe(CO)_3]_2} \qquad (1)$$

[†] Academia Sinica.

[‡] Permanent address: Department of Chemistry, University of Ilorin, Ilorin, Nigeria.

[§] National Taiwan University.

(1) (a) Whiteside, G. M.; Gaasch, J. F.; Stedronsky, E. R. *J. Am. Chem. Soc.* 1972, *94*, 5258. (b) Mann, K. R.; Morrison, W. H., Jr.; Hendrickson, D. N. *Inorg. Chem.* 1974, *13*, 1180. (c) Rudi, A. W.; Lichtenberg, D. W.; Katcher, M. L.; Davison, A. *Inorg. Chem.* 1978, *17*, 2859. (d) Hayashi, T.; Mise, T.; Fukushima, M.; Kagotani, M.; Nagashima, N.; Hamada, Y.; Matsumoto, A.; Kawakami, S.; Konishi, M.; Yamamoto, K.; Kumada, M. *Bull. Chem. Soc. Jpn.* 1980, *53*, 1138. (e) Baker, P. K.; Fraser, S. G.; Harding, P. *Inorg. Chim. Acta* 1986, *116*, L5. (f) Longato, B.; Pilloni, G.; Bonora, G. M.; Corain, B. *J. Chem. Soc., Chem. Commun.* 1986, 1478. (g) Ito, Y.; Sawamura, M.; Hayashi, T. *J. Am. Chem. Soc.* 1986, *108*, 6405. (h) Hayashi, T.; Yamamoto, A.; Hojo, M.; Ito, Y. *J. Chem. Soc., Chem. Commun.* 1989, 495.

0276-7333/92/2311-2543$03.00/0

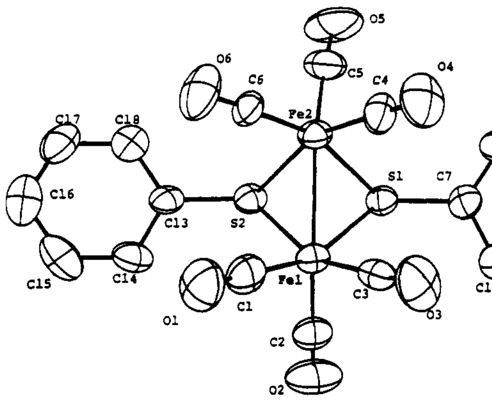

Figure 1. ORTEP molecular drawing of *syn*-$[(\mu\text{-SPh})\text{Fe(CO)}_3]_2$ (8), showing the atom-labeling scheme. Hydrogen atoms are omitted for clarity. The thermal ellipsoids are plotted at the 50% level. Selected bond lengths (Å) and angles (deg): Fe(2)⋯Fe(1), 2.495 (3); Fe(2)–S(1), 2.276 (5); Fe(2)–S(2), 2.262 (5); Fe(2)–C(4), 1.786 (19); Fe(2)–C(5), 1.799 (20); Fe(2)–C(6), 1.782 (17); Fe(1)–S(1), 2.286 (5); Fe(1)–S(2), 2.275 (5); Fe(1)–C(1), 1.787 (17); Fe(1)–C(2), 1.807 (18); Fe(1)–C(3), 1.776 (17); S(1)–C(7), 1.764 (16); S(2)–C(13), 1.787 (15); S(1)–Fe(2)–C(5), 100.5 (5); Fe(2)–S(1)–Fe(1), 66.3 (1); Fe(2)–S(1)–C(7), 114.2 (5); Fe(1)–S(1)–C(7), 116.8 (5); S(2)–Fe(2)–C(5), 100.6 (6); Fe(2)–S(2)–Fe(1), 66.7 (1); S(2)–Fe(2)–C(6), 93.5 (5); Fe(2)–S(2)–C(13), 114.4 (5); Fe(2)–Fe(1)–S(1), 56.7 (1); Fe(1)–S(2)–C(13), 115.2 (5); Fe(2)–Fe(1)–S(2), 56.4 (1).

Chart I

$[(\text{SR})\text{Fe(CO)}_3]_2$

Kinetic Product:
Syn **≡ 1,4 or 2,3 substitution**

Thermodynamic Product:
Anti **≡ 1,3 or 2,4 substitution**

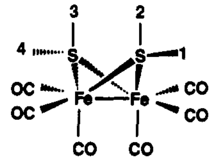

A syn form refers here to the diequatorial (or diaxial) Ph substitutions whereas an anti form refers to the axial, equatorial Ph substitutions. The diagrammatic representation of the *syn*- and the *anti*-$[(\mu\text{-SR})\text{Fe(CO)}_3]_2$ isomers is shown in Chart I. To our knowledge, successful separation of $[(\mu\text{-SPh})\text{Fe(CO)}_3]_2$ into its syn and anti isomers has not yet been achieved.[7] Only one of the isomers, the anti one, has been known for many years. This is the first time a syn isomer has been isolated and structurally characterized.

The ^{1}H NMR spectrum of *syn*-$[(\mu\text{-SPh})\text{Fe(CO)}_3]_2$ in CDCl_3 after 3 min at 42 °C shows a pattern for Ph signals different from the spectrum of freshly-made *syn*-$[(\mu\text{-SPh})\text{Fe(CO)}_3]_2$ in CDCl_3 at 25 °C. A comparison of the ^{1}H NMR spectrum (after 3 min at 42 °C) with that of an authentic sample of *anti*-$[(\mu\text{-SPh})\text{Fe(CO)}_3]_2$ in CDCl_3 reveals, surprisingly, a good match. This observation suggets that in the solution state *syn*-$[(\mu\text{-SPh})\text{Fe(CO)}_3]_2$ converts to its anti isomer, but the anti isomer does not convert back to the syn isomer. Thus, for the two $[(\mu\text{-SPh})\text{Fe(CO)}_3]_2$ isomers, the anti isomer is the thermodynamically more stable form and the syn isomer is likely a kinetic product along the reaction coordinate forming an *anti*-$[(\mu\text{-SPh})\text{Fe(CO)}_3]_2$.

For $[(\mu\text{-SMe})\text{Fe(CO)}_3]_2$, however, both syn and anti isomers have been separated and characterized without much difficulty, with the anti form being the predominant form.[8] It has been known for a long time that a tricoordinate S is able to invert itself, effectively changing the conformation of the S-containing compound.[9] The ease of separation of the *syn*- and *anti*-$[(\mu\text{-SMe})\text{Fe(CO)}_3]_2$ is most probably due to the simultaneous S-inversions of the double SMe bridges which complement the role of iron for the Fe_2S_2 core; consequently there is no interconversion between the syn- and anti-isomers. The conversion of the *syn*-$[(\mu\text{-SMe})\text{Fe(CO)}_3]_2$ to the anti form and vice versa, *via* a single S-inversion is likely to have much larger activation energy. The explanation based on the S-inversion processes is applicable to the SPh analogs, keeping in mind that a SPh group is both sterically and electronically different from a SMe group. First, the high steric energy of the diaxial Ph conformation does not favor simultaneous S-inversions for the double SPh bridges of *syn*-$[(\mu\text{-SPh})\text{Fe(CO)}_3]_2$. Second, the Ph π electrons in resonance with one of the S lone pairs would significantly decrease the activation energy for the single S-inversion. The single S-inversion process then drives the syn form to the anti form, which has favorable S-inversions for its double SPh bridges. The possibility exists for both syn and anti isomers to be present in solution, yet very briefly. Since the concentration of the anti isomer increases with time, the isolation and the X-ray diffraction study of *syn*-$[(\mu\text{-SPh})\text{Fe(CO)}_3]_2$ is a result of lucky timing in selecting the crystals fast enough.

Although detailed mechanistic studies are yet to be performed, the isolation of $(\text{C}_5\text{H}_5)\text{Fe}(\text{C}_5\text{H}_4\text{SPh})$ (3), the side product in the photolytic reaction, is apparent evidence for the C–S bond cleavage. Tentatively it is suggested that the C–S cleavage is promoted by Fe(CO)_4 coordination to S and the formation of the syn form results from steric energy of the ferrocenyl moiety at the transition state. A possible pathway initiated by Fe(CO)_4 coordination to S is shown in Scheme II. A number of reaction pathways could be proposed but no one would exclude the role of iron carbonyls in promoting the C–S bond cleavage. Recently a C–S bond cleavage producing $[(\mu\text{-SPh})\text{Fe(CO)}_3]_2$ from a photolytic reaction of PhSCH_2SPh with Fe(CO)_5 was also reported.[10] The photolytic preparation of *syn*-$[(\mu\text{-SPh})\text{Fe(CO)}_3]_2$, therefore, offers a route to the isolation of the syn isomer, where the C(Cp)–S bond of $(\text{C}_5\text{H}_4\text{SPh})_2\text{Fe}$ is apparently activated in the presence of

---

(2) Hill, D. T.; Girard, G. R.; McGabe, F. L.; Johnson, R. K.; Stupik, R. D.; Zhang, J. H.; Reiff, W. M.; Eggleston, D. S. *Inorg. Chem.* **1989**, *28*, 3529.

(3) McCulloch, B.; Ward, D. L.; Wollins, J. D.; Brubaker, C H., Jr. *Organometallics* **1985**, *4*, 1425.

(4) (a) Sato, M.; Sekino, M.; Akbori, S. *J. Organomet. Chem.* **1988**, *344*, C31. (b) Sato, M.; Sekino, M.; Katada, M.; Akbori, S. *J. Organomet. Chem.* **1989**, *377*, 327.

(5) (a) Liu, L.-K.; Yeh, S.-K.; Lin, C. C. *Bull. Inst. Chem. Acad. Sin.* **1988**, *15*, 45. (b) Kim, T.-J.; Kwon, K.-H.; Kwon, S. C.; Baeg, J.-O.; Shim, S. C.; Lee, D. H. *J. Organomet. Chem.* **1990**, *389*, 205.

(6) (a) Kettle, S. G. A.; Orgel, L. E. *J. Chem. Soc.* **1960**, 3890. (b) Ellgen, P. C.; Gerlach, J. N. *Inorg. Chem.* **1973**, *12*, 2526.

(7) (a) Maresca, L.; Greggio, F.; Sbrignadello, G.; Bor, G. *Inorg. Chim. Acta* **1971**, *5*, 667. (b) Silvio, A.; Milone, L.; Rosetti, R.; Stanghellini, P. L. *Transition Met. Chem.* **1979**, *4*, 332.

(8) King, R. B. *J. Am. Chem. Soc.* **1962**, *84*, 2460.

(9) Abel, E. W.; Long, N. J.; Orrell, K. G.; Osborne, A. G.; Sik, V.; Bates, P. A.; Hursthouse, M. B. *J. Organomet. Chem.* **1989**, *367*, 275; **1989**, *378*, 473; **1990**, *383*, 253.

(10) Raubenheimer, H. G.; Linford, L.; Lambard, A. V. A. *Organometallics* **1989**, *8*, 2062.

Scheme II

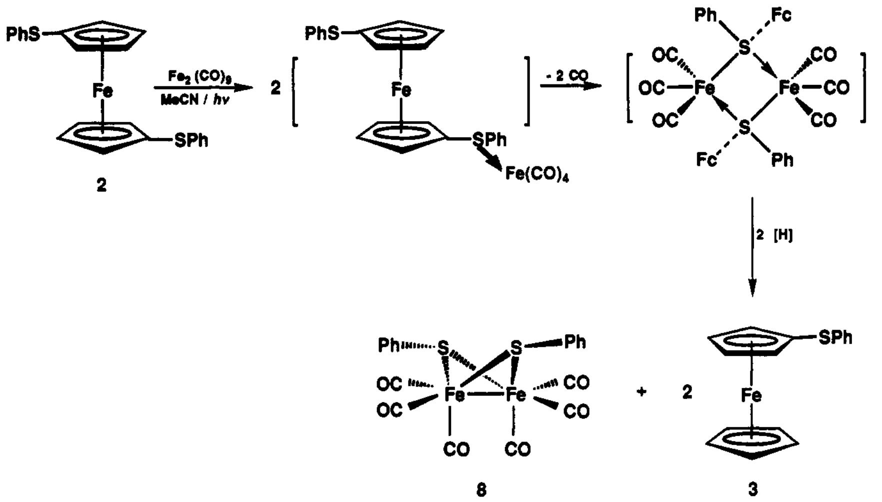

Fc=ferrocene skeleton with a SPh unit attached

$Fe_2(CO)_9$ under mild conditions forming *syn*-$[(\mu\text{-SPh})Fe(CO)_3]_2$, the kinetic product in the first instance.

The ^1H NMR spectrum of *syn*-$[(\mu\text{-SPh})Fe(CO)_3]_2$ shows only Ph proton resonances, while its IR spectrum shows ν_{CO} values at 2076 (m), 2024 (vs), 2002 (s), and 1998 (s) cm^{-1}. The side product $(C_5H_5)Fe(C_5H_4SPh)$ (**3**) has been identified by ^1H NMR spectroscopy and single-crystal X-ray diffraction. **3** has also been prepared independently *via* the selective transmetalation of $(C_5H_4SnBu_3)_2Fe$ (**4**).[11] Treatment of **4** with 1 equiv of *n*-BuLi and then PhSSPh led to $(C_5H_4SPh)Fe(C_5H_4SnBu_3$ (**5**) in 94% yield.

$$\underset{\mathbf{4}}{(C_5H_4SnBu_3)_2Fe} \xrightarrow{n\text{-BuLi}} (C_5H_4SnBu_3)Fe(C_5H_4Li) \xrightarrow{PhSSPh} \underset{\mathbf{5}}{(C_5H_4SnBu_3)Fe(C_5H_4SPh)} \quad (2)$$

Treatment of **5** with 1.05 molar equiv of *n*-BuLi followed by a quench with water produced **3** in 84% yield.

$$\mathbf{5} \xrightarrow{n\text{-BuLi}} (C_5H_4SPh)Fe(C_5H_4Li) \xrightarrow{H_2O} \mathbf{3} \quad (3)$$

The physical data are consistent with those obtained in the photolytic reaction.

Since the selective transmetalation reaction was successful, extension has been attempted in designing ferrocenyl ligands with S donor atoms on one Cp ring and P on the other. The preparation of $(C_5H_4SPh)Fe(C_5H_4PPh_2$ (**7**) is conducted, and it is the first example of a ferrocene skeleton having both S and P donor atoms. Selective transmetalation of **4** with 1 molar equiv of *n*-BuLi, followed by treatment with PPh_2Cl, gave $(C_5H_4PPh_2)Fe(C_5H_4SnBu_3)$ (**6**).

$$\mathbf{4} \xrightarrow{n\text{-BuLi}} (C_5H_4SnBu_3)Fe(C_5H_4Li) \xrightarrow{PPh_2Cl} \underset{\mathbf{6}}{(C_5H_4SnBu_3)Fe(C_5H_4PPh_2)} \quad (4)$$

Subsequent treatment of **6** with 1 equiv of *n*-BuLi, followed by PhSSPh, gave the new ligand **7** in 85% yield.

$$\mathbf{6} \xrightarrow{n\text{-BuLi}} (C_5H_4Li)Fe(C_5H_4PPh_2) \xrightarrow{PhSSPh} \underset{\mathbf{7}}{(C_5H_4SPh)Fe(C_5H_4PPh_2)} \quad (5)$$

As a whole, the syntheses of **2**, **3**, **5**, **6**, and **7** are shown in Scheme I.

The ^1H NMR spectra of the ferrocenyl derivatives **3**, **5**, and **7** show a similar pattern for the SPh-substituted Cp proton resonances. For **3** the $H_{2,5}$ and $H_{3,4}$ peaks are at δ 4.39 and 4.32, for **5** they are at δ 4.45 and 4.34, and for **7** they are at δ 4.45 and 4.29, respectively. The singlet at δ 4.25 in **3** is due to the five protons of unsubstituted Cp ring. Considering the $SnBu_3$-substituted Cp ring, the $H_{2,5}$ and $H_{3,4}$ protons in are observed upfield at δ 4.23 and 3.95 in **4**, at δ 4.27 and 4.09 in **5**, and at δ 4.03 and 3.92 in **6**, respectively. The $H_{2,5}$ and $H_{3,4}$ proton resonances for the PPh_2-substituted Cp ring are found in between, higher than for the SPh-substituted ones and lower than for the $SnBu_3$-substituted ones, at δ 4.29 and 4.21 for **6** and at δ 4.21 and 4.18 for **7**, respectively. This result is consistent with the relative shielding or deshielding effect of the S, P, and Sn atoms.

The ipso-C atoms of SPh in **3**, **5**, and **7** are found for the ^{13}C NMR measurements at δ 140.77, 141.02, and 140.44, while the ipso-C atoms of SCp are found at δ 75.63, 77.62, and 77.21, respectively. The C atoms of the unsubstituted Cp ring in **3** resonate at δ 69.61. The $^{31}P\{^1H\}$ NMR spectrum of **7** shows one signal at δ −16.88. The mass spectrum of **7** shows molecular fragments resulting from loss of a SPh unit. The mass spectra of **3** and **5** exhibit the molecular ion with M^+ also being the most intense peak.

In a separate experiment we have attempted to prepare compound **7** by treating $(C_5H_4Li)_2Fe$ (**1**) with $PhSPPh_2$.[12] Instead of **7**, $(C_5H_4PPh_2)_2Fe$, dppf, [13] was obtained as the main product.

$$\underset{\mathbf{1}}{(C_5H_4Li)_2Fe} + 2PhSPPH_2 \rightarrow (C_5H_4PPH_2)_2Fe + 2LiSPh \quad (6)$$

This result shows that the nucleophilic cleavage of the P–S bond, leaves the PPh_2, not the SPh, attached to the Cp ring. Consequently the two Cp rings become functionalized by the P donor atoms. The synthetic applicability of $RSPR'_2$ to other systems is currently being explored.

X-ray Structure Analysis. The molecular structure of *syn*-$[(\mu\text{-SPh})Fe(CO)_3]_2$ (**8**) (see Figure 1) shows the presence of a nonpolar Fe_2S_2 core in a butterfly form, with both Ph groups being seen in the equatorial positions. The Fe–Fe distance of 2.495 (3) Å confirms the presence of a Fe–Fe bond. The Fe–S–Fe bridge angles are approxi-

---

(11) Wright, M. E. *Organometallics* **1990**, *9*, 853.

(12) Job, B. E.; Mclean, R. A. N.; Thompson, D. T. *J. Chem. Soc., Chem. Commun.* **1966**, 895.

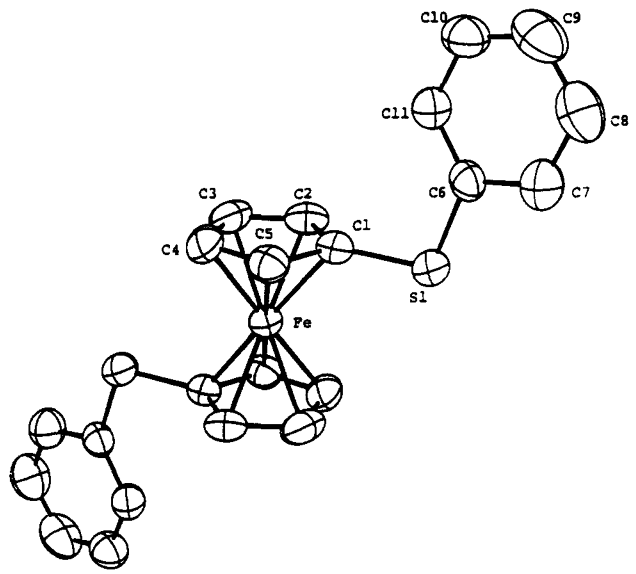

Figure 2. ORTEP molecular drawing of $(C_5H_4SPh)_2Fe$ (2), showing the atom-labeling scheme. Hydrogen atoms are omitted for clarity. The thermal ellipsoids are plotted at the 50% level. Selected bond lengths (Å) and angles (deg): Fe–C(1), 2.023 (2); Fe–C(2), 2.034 (2); Fe–C(3), 2.040 (2); Fe–C(4), 2.043 (2); Fe–C(5), 2.037 (2); S(1)–C(1), 1.753 (2); S(1)–C(6), 1.769 (2); C(1)–C(2), 1.425 (3); C(1)–C(5), 1.418 (3); C(2)–C(3), 1.404 (3); C(4)–C(5), 1.405 (3); C(6)–C(7), 1.394 (3); C(7)–C(8), 1.378 (4); C(8)–C(9), 1.370 (5); C(9)–C(10), 1.362 (4); S(1)–C(1)–C(2), 126.7 (2); S(1)–C(1)–C(5), 125.5 (2); S(1)–C(6)–C(7), 117.0 (2); S(1)–C(6)–C(11), 123.8 (2); C(1)–S(1)–C(6), 102.6 (1); Fe–C(1)–S(1), 121.9 (1).

mately 66.5°. 8 is formed by the intersection of the basal planes of two distorted tetragonal pyramids (dibasal *cis*-$Fe(CO)_3S_2$) along the S···S line with a dihedral angle of 63.3°. Dahl has suggested that a "bent" metal–metal bond[14] involving the overlap of octahedral Fe orbitals is presumably responsible for the molecular geometry of a structurally similar $[(\mu\text{-}SC_2H_5)Fe(CO)_3]_2$ with the Fe–S–Fe bridge angle of 68°. The structure of 8 is not significantly different in bond distances and bond angles from the structure of the *anti*-$[(\mu\text{-}SPh)Fe(CO)_3]_2$. [The Fe–Fe length is 2.516 (2) Å; the Fe–S–Fe angles are approximately 67°; the two basal planes of tetragonally pyramidal $Fe(CO)_3S_2$ have a dihedral angle 66.5°.][15] In the crystalline state, the syn form retains an approximately C_{2v} molecular symmetry, which the anti form does not have.

The molecule of 2 is centrosymmetric with the ferrocenyl Fe atom at a crystallographic inversion center. The ORTEP plot of 2 is shown in Figure 2, the Cp rings being staggered and parallel. The two S donor atoms appear on opposite sides of the Cp ring in a similar fashion found for the two P atoms in the centrosymmetric dppf.[16] The SPh group is planar within 0.001 Å and is almost orthogonal to the attached Cp ring with a dihedral angle between them as 86.7°. All bond lengths are typical of a substituted ferrocene[17] with the Fe–C bonds averaging 2.036 (2) Å. The C–C bonds of Cp are in the range 1.404–1.425 Å. The S–C(Cp) bond, 1.753 (2) Å, is shorter than the S–C(Ph) bond, 1.769 (2) Å. The inner ring angle at the ipso-C atom of Cp is 107.7 (2)° with the rest averaging 108.1°. The distance between the centroids of the Cp rings is calculated to be 3.286 Å.

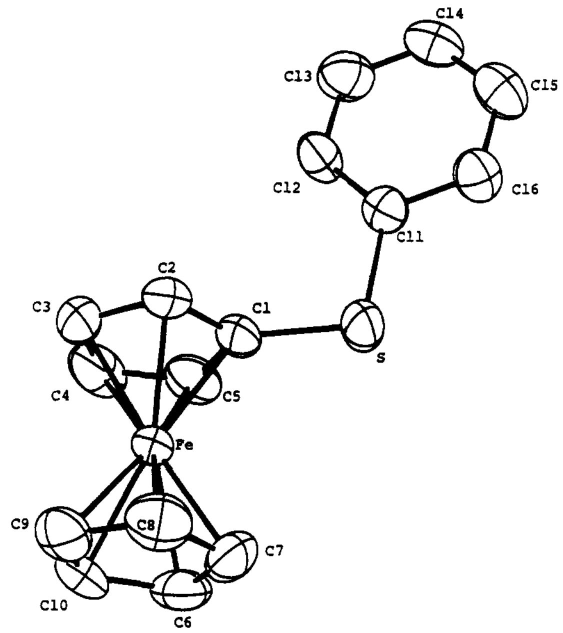

Figure 3. ORTEP molecular drawing of $(C_5H_5)Fe(C_5H_4SPh)$ (3), showing the atom-labeling scheme. Hydrogen atoms are omitted for clarity. The thermal ellipsoids are plotted at the 50% level. Selected bond lengths (Å) and angles (deg): Fe–C(1), 2.024 (5); Fe–C(2), 2.022 (5); Fe–C(3), 2.022 (5); Fe–C(4), 2.020 (7); Fe–C(5), 2.029 (6); Fe–C(6), 2.033 (6); Fe–C(7), 2.028 (5); Fe–C(8), 2.036 (6); Fe–C(9), 2.033 (5); Fe–C(10), 2.030 (5); S–C(1), 1.749 (5); C(1)–C(2), 1.420 (8); C(1)–C(5), 1.420 (7); C(2)–C(3), 1.396 (9); C(3)–C(4), 1.387 (13); C(4)–C(5), 1.428 (10); C(6)–C(7), 1.397 (10); C(6)–C(10), 1.407 (9); C(7)–C(8), 1.411 (9); C(8)–C(9), 1.399 (9); C(9)–C(10), 1.400 (9); C(1)–S–C(11), 102.8 (2); S–C(1)–C(2), 125.3 (4); S–C(1)–C(5), 127.0 (5); S–C(11)–C(12), 124.6 (4); S–C(11)–C(16), 116.4 (4); Fe–C(1)–S, 126.9 (3).

Shown in Figure 3, the molecule of 3 is −1.7° from a fully eclipsed conformation and the planar Cp rings are essentially parallel, the angle between plane normals being 2.4 (3)°. The SPh plane is almost perpendicular to the attached Cp plane with interplanar angle of 93.5 (3)°. The Fe–C bonds average 2.025 (6) Å to the SPh-substituted Cp ring and 2.036 (6) Å to the unsubstituted Cp ring. The C–C bond lengths in the SPh-substituted Cp ring average 1.413 (10) Å, while the C–C bond lengths in the unsubstituted ring average 1.406 (10) Å. The S–C bonds of 1.750 (6) Å to Cp ring and of 1.788 (6) Å to Ph ring are similar to those in 2. The C–C–C angle of the Cp ring at the substituted C atom is 107.3 (5)°, the rest averaging 108.2°. The distance between the Cp centroids is calculated to be 3.276 Å.

The molecular structure of 7 is shown in Figure 4. It has a slightly distorted eclipsed conformation (5.9° from fully eclipsed). The Cp rings are planar and parallel. The SPh and one of the PPh groups are almost perpendicular to the respectively attached Cp planes. The dihedral angle between SPh and the attached Cp plane is 97.9 (6)°. The interplanar angle between the plane defined by P, C(23)–C(28), and the attached Cp plane is 95.9°. The C–C bond lengths on the SPh-substituted Cp ring average 1.415 Å, while those on the PPh_2-substituted Cp ring average 1.414 Å. For SPh-substituted Cp, the inner ring angle of the ipso-C atom is 107.7 (3)° with the rest averaging 108.1°. For PPh_2-substituted Cp, the corresponding angles are 108.4 (3) and 107.9°, respectively. The distance between the centroids of the Cp rings is 3.310 Å, slightly larger than in 2 and 3.

---

[13] Bishop, J. J.; Davison, A.; Katcher, M. L.; Lichtenberg, D. W.; Merrill, R. E.; Smart, J. C. *J. Organomet. Chem.* **1971**, *27*, 242.

[14] Dahl, L. F.; Wei, C.-H. *Inorg. Chem.* **1963**, *2*, 328.

[15] Henslee, W.; Davis, R. E. *Cryst. Struct. Commun.* **1972**, *1*, 403.

[16] Casellato, U.; Ajo, D.; Valle, G.; Corain, B.; Longato, B.; Graciani, R. *J. Crystallogr. Spectrosc. Res.* **1988**, *18*, 583.

[17] (a) Gunther, H. *NMR Spectroscopy*; Wiley: New York, 1980; p 184. (b) Bruce, M. I. In *Comprehensive Organometallic Chemistry*; Wilkinson, G., Stone, F.G.A., Abel, E. W., Eds.; Pergamon Press: Oxford, U.K., 1982; Vol. 9, p 1294 and references therein.

Table I. Crystal Data and Refinement Details for 2, 3, 7, and 8

compd	2	3	7	8
empirical formula	$C_{22}H_{18}FeS_2$	$C_{16}H_{14}FeS$	$C_{28}H_{23}FeSP$	$C_{18}H_{10}Fe_2O_6S_2$
fw	402.35	294.19	478.37	498.08
cryst system	monoclinic	orthorhombic	triclinic	orthorhombic
space group	$P2_1/c$	$P2_12_12_1$	$P\bar{1}$	*Pbca*
a, Å	6.099 (3)	7.307 (8)	9.675 (2)	7.151 (2)
b, Å	7.885 (1)	9.0180 (9)	10.903 (4)	20.847 (3)
c, Å	19.027 (3)	20.033 (3)	12.899 (3)	27.155 (4)
α, deg	90	90	112.89 (3)	90
β, deg	98.21 (2)	90	86.89 (2)	90
γ, deg	90	90	113.53 (2)	90
V, Å^3	902.2 (4)	1320.1 (3)	1141.0 (5)	4048.0 (1)
cell const determination				
no. of reflns	25	25	24	25
2θ range, deg	15.80–33.74	18.86–32.92	18.78–34.22	7.94–26.18
Z	2	4	2	8
$F(000)$	415.94	607.91	991.86	1999.70
D_{calc}, g/cm^3	1.481	1.480	1.392	1.635
μ, mm^{-1}	1.06	1.27	1.66	1.66
λ, Å	0.7093	0.7093	0.7093	0.7093
cryst dim, mm	0.49 × 0.31 × 0.25	0.26 × 0.19 × 0.25	0.41 × 0.26 × 0.26	0.28 × 0.20 × 0.13
2θ(max), deg	60	50	45	50
diffractometer	Nonius CAD4			
scan mode	$\theta/2\theta$			
scan range				
h	−8 to 8	0 to 8	−10 to 9	0 to 8
k	0 to 11	0 to 10	0 to 11	0 to 24
l	0 to 26	0 to 23	−13 to 12	0 to 32
no. of reflns measd	2616	1368	2983	3534
no. of reflns obsd	1976, $I > 2.5\sigma(I)$	1054, $I > 2.5\sigma(I)$	2567, $I > 2.5\sigma(I)$	1247, $I > 2.5\sigma(I)$
abs corr	yes	yes	yes	no
trans factor	0.971–1.000	0.949–0.998	0.950–1.000	
no. of atoms	22	32	54	38
no. of params	152	220	280	253
weighting	counting statistics			
K factor	0.01	0.01	0.01	0.014
R	0.029	0.026	0.032	0.043
R_w	0.035	0.028	0.040	0.043
GOF	1.73	1.18	2.15	1.20
Δ/σ	0.000	0.017	0.008	0.008
resid peak, e/Å^3	0.250	0.200	0.210	0.380
resid hole, e/Å^3	−0.260	−0.220	−0.290	−0.310

The rotational barrier of ferrocene from the eclipsed form to the staggered form has been reported experimentally to range from 3.8 (1.3) kJ mol^{-1} (in the gas phase by electron diffraction) to 7.5–9.6 kJ mol^{-1} (in the low-temperature crystal).[18] These barriers are not large and are likely overrun by the substituent effects in conjunction with crystal packing. The molecule **2** displays a staggered form whereas **3** and **7** have an eclipsed form in the solid state.

In the solid state, both **2** and dppf[16] possess a crystallographic center of symmetry at Fe. Both have a fully staggered conformation and parallel Cp rings. **7** stands midway between **2** and dppf. Its structural parameters of the SPh-substituted Cp ring have been found to be similar to these found in **2**, with the SPh group being approximately orthogonal to the attached Cp ring, as in **2**. At the PPh_2-substituted Cp ring of **7**, the bond distances and angles including those around P have been found to be similar to those found in dppf. One of the Ph groups in PPh_2 lies almost orthogonal to the attached Cp plane in **7**, the same as in dppf. The almost perpendicular orientation of SPh or PPh to the Cp plane may be due less to the mode of stacking in the unit cell but mainly to the electronic effect of the S or P lone pair in resonance with Ph ring current. The ferrocenyl moiety has a relatively large electron density on its Cp rings in the π-cloud, and consequently large repulsion between the lone pair on S or P and the π-cloud on Cp is expected.

Experimental Section

Unless otherwise stated all reactions were routinely performed under an inert atmosphere of dry nitrogen. Reactions involving phosphines and other air- and moisture-sensitive compounds were carried out using a drybox or Schlenk and standard vacuum line techniques. ^1H (200 MHz), $^{13}\{^1H\}$ (50.33 MHz), and $^{31}P\{^1H\}$ (81 MHz) NMR spectra were recorded on a Bruker MSL 200 or a Bruker AC 200 FT spectrophotometer with chemical shifts in δ units relative to Me_4Si (^1H, δ 0.00), $CDCl_3$ (^{13}C, δ 77.0), and external H_3PO_4 (85%, ^{31}P, δ 0.00), respectively. The infrared spectra were recorded on a Perkin-Elmer 882 spectrophotometer with CaF_2 optics. Low-resolution mass spectroscopy spectra were recorded on a VG 70-250S mass spectrometer. Melting points were determined on a Yanaco micro melting point apparatus, and values were uncorrected. Elemental analyses were performed on a Perkin-Elmer 2400 CHN elemental analyzer as operated by the Institute of Chemistry, Academia Sinica.

$Fe_2(CO)_9$[19] and $(C_5H_4Li)_2Fe$ were prepared according to a modified literature procedure. *n*-BuLi (1.6 M in hexane) and all other chemicals were purchased from Aldrich Chemical Co. or E. Merck Co. and used without further purification. THF, diethyl ether, hexane, and benzene were distilled from sodium or potassium benzophenone ketyl. MeCN was refluxed and distilled from P_2O_5.

Preparation of 1,1′-Bis(phenylthio)ferrocene (2). *N*,*N*,-*N*′,*N*′-tetramethylethylenediamine (TMEDA) (8.5 mL, 54.6 mmol) and *n*-BuLi (34.1 mL, 54.6 mmol) were added dropwise from a pressure-equalizing dropping funnel to a stirred solution of

---

(18) Deeming, A. J. In *Comprehensive Organometallic Chemistry*; Wilkinson, G., Stone, F. G. A., Abel, E. W., Eds.; Pergamon Press: Oxford, U.K., 1982; Vol. 4, pp 478–479.

(19) Braye, E. H.; Hubel, W. *Inorg. Synth.* **1966**, *8*, 178.

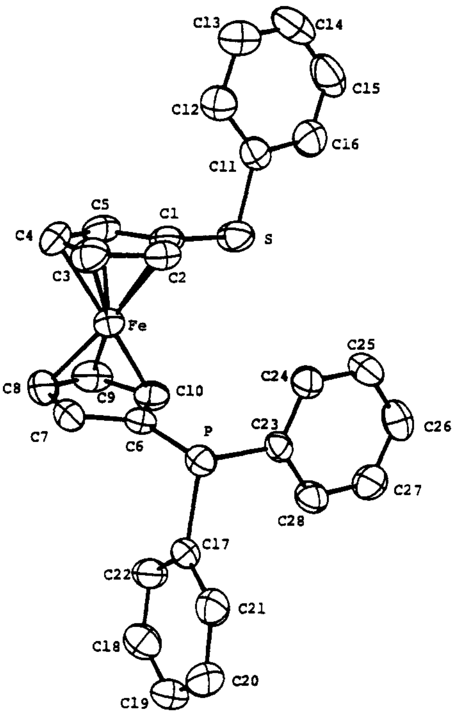

Figure 4. ORTEP molecular drawing of $(C_5H_4SPh)Fe(C_5H_4PPh_2)$ (7), showing the atom-labeling scheme. Hydrogen atoms are omitted for clarity. The thermal ellipsoids are plotted at the 50% level. Selected bond lengths (Å) and angles (deg): Fe–C(1), 2.031 (3); Fe–C(2), 2.063 (3); Fe–C(3), 2.055 (3); Fe–C(4), 2.042 (3); Fe–C(5), 2.026 (3); Fe–C(6), 2.068 (3); Fe–C(7), 2.046 (3); Fe–C(8), 2.040 (3); Fe–C(9), 2.040 (3); Fe–C(10), 2.052 (3); P–C(6), 1.814 (3); P–C(17), 1.831 (3); P–C(23), 1.834 (3); S–C(1), 1.748 (3); S–C(11), 1.774 (3); C(1)–C(5), 1.433 (5); C(1)–C(2), 1.420 (4); C(3)–C(4), 1.413 (5); C(4)–C(5), 1.411 (5); C(6)–C(7), 1.432 (5); C(6)–C(10), 1.423 (4); C(7)–C(8), 1.418 (5); C(8)–C(9), 1.399 (6); C(9)–C(10), 1.416 (5); P–C(6)–C(7), 122.8 (23); P–C(6)–C(10), 130.5 (2); P–C(17)–C(22), 124.1 (2); P–C(23)–C(24), 117.8 (2); P–C(23)–C(28), 124.2 (2); C(6)–P–C(17), 101.2 (1); C(6)–P–C(23), 101.5 (1); C(17–P–C(23), 101.0 (1); S–C(1)–C(2), 126.6 (3); S–C(1)–C(5), 125.7 (3); S–C(11)–C(12), 124.8 (3); S–C(11)–C(16) 116.2 (3); Fe–C(1)–S, 124.4 (2).

Table II. Final Fractional Coordinates and B_{iso} Values ($Å^2$) for *syn*-$[(\mu\text{-}SPh)Fe(CO)_3]_2$ (8)

atom	*x*	*y*	*z*	B_{iso}
Fe2	0.5376 (3)	0.4650 (1)	0.0906 (1)	3.24 (10)
Fel	0.3489 (3)	0.4269 (1)	0.1621 (1)	3.43 (11)
S1	0.5873 (5)	0.4995 (2)	0.1690 (1)	3.5 (2)
S2	0.6082 (6)	0.3755 (2)	0.1339 (1)	3.4 (2)
O1	0.0867 (17)	0.3446 (6)	0.1093 (5)	6.6 (8)
O2	0.3400 (22)	0.3662 (7)	0.2593 (5)	8.9 (9)
O3	0.0630 (16)	0.5262 (6)	0.1679 (5)	6.7 (7)
O4	0.3160 (19)	0.5760 (6)	0.0598 (5)	6.7 (8)
O5	0.9080 (20)	0.4915 (7)	0.0479 (5)	7.9 (9)
O6	0.3415 (20)	0.3959 (6)	0.0125 (4)	6.9 (8)
C1	0.1896 (23)	0.3753 (8)	0.1305 (6)	4.4 (9)
C2	0.3417 (26)	0.3907 (9)	0.2226 (7)	5.1 (10)
C3	0.1721 (23)	0.4866 (8)	0.1656 (7)	4.4 (8)
C4	0.4063 (26)	0.5340 (9)	0.0726 (6)	4.7 (10)
C5	0.7610 (28)	0.4825 (8)	0.0633 (6)	4.4 (10)
C6	0.4254 (22)	0.4213 (8)	0.0425 (6)	3.8 (8)
C7	0.5236 (21)	0.5801 (7)	0.1793 (5)	3.4 (8)
C8	0.3853 (25)	0.6596 (10)	0.2321 (7)	5.3 (10)
C9	0.4468 (27)	0.7083 (9)	0.2015 (8)	5.5 (11)
C10	0.5512 (27)	0.6919 (9)	0.1610 (8)	5.8 (11)
C11	0.4212 (22)	0.5966 (8)	0.2208 (6)	3.8 (8)
C12	0.5880 (23)	0.6282 (9)	0.1495 (6)	4.5 (9)
C13	0.5647 (22)	0.3022 (7)	0.1018 (6)	3.7 (8)
C14	0.4694 (24)	0.2530 (9)	0.1242 (6)	5.0 (9)
C15	0.4470 (27)	0.1940 (8)	0.0999 (8)	6.1 (12)
C16	0.5286 (31)	0.1862 (10)	0.0551 (8)	6.4 (12)
C17	0.6266 (28)	0.2333 (10)	0.0335 (7)	5.8 (11)
C18	0.6514 (24)	0.2920 (8)	0.0569 (6)	4.5 (9)
H8	0.3060	0.6715	0.2668	5.8
H9	0.4128	0.7586	0.2101	6.3
H10	0.6041	0.7310	0.1366	6.4
H11	0.3675	0.5574	0.2461	4.7
H12	0.6714	0.6163	0.1159	5.2
H14	0.4103	0.2594	0.1623	5.8
H15	0.3710	0.1536	0.1185	7.0
H16	0.5101	0.1393	0.0363	6.9
H17	0.6847	0.2260	−0.0043	6.4
H18	0.7407	0.3303	0.0400	5.4

$(C_5H_5)_2Fe$ (5 g, 26.9 mmol) in hexane (100 mL) under a dry N_2 atmosphere. The solution was stirred overnight. The orange slurry was allowed to settle and the hexane layer transferred *via* cannula. The orange powder left was washed with hexane (3 × 20 mL) to remove excess *n*-BuLi and unreacted $(C_5H_5)_2Fe$. PhSSPh (4 g, 110 mmol) in dry benzene (100 mL) was added dropwise to the suspension of the above yellow solid $(C_5H_4Li)_2Fe$ (1) in hexane (50 mL) at -10 °C. The reaction mixture was stirred overnight at room temperature to give a yellow suspension, which was filtered on a sintered glass funnel and then washed with water (30 mL) and hexane (2 × 20 mL). Recrystallization from CH_2Cl_2 gave $(C_5H_4SPh)_2Fe$ as needle crystals (17.1 g, 42 mmol, 78%), mp 172–173 °C (lit.[3] yield 80%, mp 172–173 °C).

Reaction of 2 with $Fe_2(CO)_9$ under Photolytic Conditions. At 25 °C, 2 (0.402 g, 1.0 mmol) and $Fe_2(CO)_9$ (0.182 g, 0.5 mmol) were dissolved in MeCN (80 mL). The yellow suspension was irradiated with a medium-pressure Hg lamp for ca. 48 h, during which the solution changed from yellow to dark-red. The solvent was removed on a rotary evaporator to give a dark-red solid, which was chromatographed on silica with *n*-hexane and then ethyl acetate/*n*-hexane (1:12) as eluent. The first dark-red band was collected and identified to be *syn*-$[(\mu\text{-}SPh)Fe(CO)_3]_2$ (0.05 g, 0.1 mmol, 20%), mp 131–135 °C. ^1H NMR ($CDCl_3$): δ 7.52–7.02 (m). IR (ν(CO), in hexane): 2076 (m), 2042 (s), 2002 (m), 1998 (s) cm^{-1}. The yellow band that eluted next was identified to be $(C_5H_5)Fe(C_5H_4SPh)$ (3) (0.117 g, 3.98 mmol, 40%), mp 107–109 °C. ^1H NMR ($CDCl_3$): δ 7.17–7.02 (m, 5 H), 4.39 (t, 2 H, *J* = 1.9 Hz), 4.33 (t, 2 H, *J* = 1.9 Hz), 4.25 (s, 5 H). MS: *m/e* 294 [M^+].

Preparation of 1,1′-Bis(tri-*n*-butylstannyl)ferrocene (4). A *n*-hexane (50 mL) slurry of $(C_5H_4Li)_2Fe$ (1) (26.5 mmol) was treated with Bu_3SnCl (18.4 g, 54 mmol) at 0 °C. The reaction mixture was allowed to warm to ambient temperature and stirred overnight. The hexane layer was diluted with hexane (50 mL) and washed with water (50 mL) and brine (2 × 50 mL) and then dried over K_2CO_3. The solvent was removed, and the residual oil (20.2 g) was run through a column of nonactivated Al_2O_3 in batches with hexane as eluent. The first orange band was collected and the solvent removed to afford $(C_5H_4SnBu_3)_2Fe$ (4) as a red oil (13.7 g, 18 mmol; 67.3%, lit.[11] yield 68%). ^1H NMR ($CDCl_3$): δ 4.23 (t, *J* = 1.6 Hz, 4 H), 3.95 (t, *J* 1.6 Hz, 4 H) 1.65–1.49 (m, 6 H), 1.44–1.26 (m, 6 H), 1.05–0.96 (m, 6 H), 0.91 (t, *J* = 7.1 Hz, 9 H). ^{13}C NMR ($CDCl_3$): δ 74.20, 70.45, 67.92 (Cp), 29.22, 27.42, 13.71, 10.25 (Bu). MS: *m/e* 764 [M^+, 100%], 706 [M^+ - Bu, 10%], 476 [M^+ - $SnBu_3$, 20%], 419 [M^+ - $SnBu_4$, 10%], 361 [M^+ - $SnBu_5$, 3%]. Anal. Calcd for $C_{34}H_{62}FeSn_2$: C, 53.44; H, 8.18. Found: C, 53.67; H, 8.19.

Preparation of 1-(Tri-*n*-butylstannyl)-1′-(phenylthio)ferrocene (5). *n*-BuLi (4.0 mL, 6.4 mmol) was added dropwise to a THF (40 mL) solution of 4 (4.89 g, 6.4 mmol) at -78 °C. The reaction mixture was stirred for a further 30 min. To the orange-red solution was added PhSSPh (1.4 g, 6.4 mmol) in THF (10 mL). The cooling bath was removed, and the reaction mixture was diluted with ether (100 mL) and washed with water (100 mL) and then brine (2 × 50 mL). The organic layer was dried, and the solvents were removed in vacuo. The crude red oil was chromatographed on Al_2O_3 with hexane as eluent. The first band was identified to be unreacted 4 (0.12 g). The second band was identified to be $(C_5H_4SPh)Fe(C_5H_4SnBu_3)$ (5) (3.5 g, 60 mmol, 94%). ^1H NMR ($CDCl_3$): δ 7.51–7.00 (m, 5 H), 4.45 (t, *J* = 1.7 Hz, 2 H), 4.34 (t, *J* = 1.8 Hz, 2 H), 4.27 (t, *J* = 1.8 Hz, 2 H), 4.09 (q, *J* = 1.7 Hz, 2 H), 1.62–1.41 (m, 6 H), 1.39–1.23 (m, 6 H), 1.09–1.01 (m, 6 H), 0.91 (t, *J* = 7.1 Hz, 9 H). ^{13}C NMR ($CDCl_3$): δ 141.02 (s, ipso Ph), 128.53 (Ph), 125.73 (Ph), 124.71 (Ph), 77.62 (ipso Cp), 76.05 (CpS), 74.87 (CpSn), 72.22 (CpSn), 70.09 (CpS), 29.17, 27.41, 13.71, 10.29 (Bu). MS: *m/e* 583 [M^+, 95%], 584 [(M

Table III. Final Fractional Coordinates and B_{iso} Values (Å^2) for $(C_5H_4SPh)_2Fe$ (2)

atom	*x*	*y*	*z*	B_{iso}
Fe	0.00000	0.00000	0.00000	2.92 (1)
S1	0.26450 (9)	0.35722 (7)	0.04889 (3)	4.33 (2)
C1	0.0829 (3)	0.1958 (2)	0.0676 (1)	3.3 (1)
C2	−0.1509 (3)	0.1916 (3)	0.0468 (1)	3.9 (1)
C3	−0.2271 (4)	0.0335 (3)	0.0677 (1)	4.5 (1)
C4	−0.0446 (4)	−0.0609 (3)	0.1014 (1)	4.4 (1)
C5	0.1464 (4)	0.0394 (3)	0.1018 (1)	3.6 (1)
C6	0.2868 (3)	0.4853 (2)	0.1261 (1)	3.6 (1)
C7	0.4709 (4)	0.5917 (3)	0.1391 (1)	4.8 (1)
C8	0.4970 (5)	0.6955 (3)	0.1982 (2)	5.8 (1)
C9	0.3441 (5)	0.6935 (3)	0.2443 (1)	5.9 (1)
C10	0.1630 (5)	0.5906 (3)	0.2317 (1)	5.0 (1)
C11	0.1331 (4)	0.4863 (3)	0.1723 (1)	4.1 (1)
H1	0.294 (4)	0.007 (2)	0.122 (1)	4.1 (5)
H2	−0.228 (3)	0.279 (3)	0.023 (1)	3.9 (4)
H3	−0.365 (5)	−0.003 (3)	0.063 (1)	6.3 (7)
H8	0.051 (4)	0.593 (3)	0.261 (1)	5.6 (6)
H9	0.016 (3)	0.423 (3)	0.162 (1)	4.1 (5)
H4	−0.050 (4)	−0.177 (3)	0.118 (1)	6.3 (6)
H5	0.577 (4)	0.588 (3)	0.108 (1)	6.0 (6)
H6	0.616 (4)	0.764 (4)	0.208 (1)	7.2 (7)
H7	0.362 (4)	0.756 (4)	0.284 (1)	7.2 (7)

Table IV. Final Fractional Coordinates and B_{iso} Values (Å^2) for $(C_5H_5)Fe(C_5H_4SPh)$ (3)

atom	*x*	*y*	*z*	B_{iso}
Fe	0.09015 (9)	0.00907 (7)	0.07714 (3)	3.03 (3)
S	0.07452 (19)	−0.32301 (15)	0.15497 (7)	4.47 (6)
C1	0.1899 (7)	−0.1888 (6)	0.1081 (3)	3.5 (2)
C2	0.2950 (8)	−0.0704 (6)	0.1348 (3)	4.4 (3)
C3	0.3665 (7)	0.0101 (8)	0.0813 (5)	5.9 (4)
C4	0.3084 (10)	−0.0524 (9)	0.0218 (4)	5.9 (4)
C5	0.1981 (9)	−0.1784 (7)	0.0374 (3)	4.6 (3)
C6	−0.1598 (8)	0.0430 (7)	0.0353 (3)	4.9 (3)
C7	−0.1759 (7)	0.0289 (8)	0.1045 (3)	4.6 (3)
C8	−0.0715 (9)	0.1436 (7)	0.1336 (3)	5.0 (3)
C9	0.0110 (8)	0.2249 (6)	0.0822 (4)	4.4 (3)
C10	−0.0429 (8)	0.1629 (7)	0.0213 (3)	4.2 (3)
C11	0.2508 (7)	−0.4550 (5)	0.1731 (2)	3.4 (2)
C12	0.4250 (9)	−0.4511 (6)	0.1464 (3)	4.0 (2)
C13	0.5482 (9)	−0.5614 (8)	0.1625 (3)	5.1 (3)
C14	0.5003 (10)	−0.6765 (8)	0.2040 (3)	4.6 (3)
C15	0.3288 (10)	−0.6791 (7)	0.2310 (3)	4.7 (3)
C16	0.2039 (8)	−0.5700 (6)	0.2157 (3)	4.1 (3)
H2	0.296 (8)	−0.050 (6)	0.183 (3)	7.6 (19)
H3	0.433 (7)	0.093 (5)	0.089 (3)	4.7 (13)
H4	0.325 (8)	−0.045 (7)	−0.019 (3)	6.4 (19)
H5	0.128 (7)	−0.240 (6)	0.006 (3)	5.2 (14)
H6	−0.215 (7)	−0.019 (7)	0.007 (2)	5.1 (14)
H7	−0.245 (6)	−0.046 (5)	0.125 (2)	3.4 (11)
H8	−0.060 (7)	0.168 (6)	0.180 (2)	5.4 (13)
H9	0.087 (8)	0.307 (6)	0.085 (3)	6.6 (15)
H10	−0.011 (8)	0.195 (7)	−0.022 (3)	6.6 (16)
H12	0.453 (6)	−0.387 (5)	0.119 (2)	3.0 (11)
H13	0.658 (6)	−0.550 (5)	0.145 (2)	3.6 (12)
H14	0.600 (9)	−0.749 (7)	0.216 (3)	8.3 (18)
H15	0.287 (8)	−0.762 (6)	0.258 (3)	6.0 (15)
H16	0.085 (5)	−0.571 (5)	0.234 (2)	3.0 (10)

Table V. Final Fractional Coordinates and B_{iso} Values (Å^2) for $(C_5H_4SPh)Fe(C_5H_4PPh_2)$ (7)

atom	*x*	*y*	*z*	B_{iso}
Fe	0.26010 (5)	0.73696 (5)	0.23336 (4)	3.10 (3)
P	0.31629 (10)	0.62434 (9)	−0.05362 (7)	2.93 (5)
S	0.60809 (10)	0.82220 (10)	0.34297 (8)	4.55 (6)
C1	0.4115 (4)	0.7228 (3)	0.3264 (3)	3.4 (2)
C2	0.3259 (4)	0.5823 (3)	0.2412 (3)	3.3 (2)
C3	0.1706 (4)	0.5453 (4)	0.2568 (3)	4.0 (2)
C4	0.1596 (4)	0.6607 (4)	0.3522 (3)	4.4 (2)
C5	0.3073 (4)	0.7708 (4)	0.3959 (3)	4.1 (2)
C6	0.2756 (3)	0.7448 (3)	0.0754 (2)	2.9 (2)
C7	0.1250 (4)	0.7173 (4)	0.1060 (3)	3.7 (2)
C8	0.1327 (4)	0.8356 (4)	0.2079 (3)	4.7 (3)
C9	0.2847 (5)	0.9351 (4)	0.2409 (3)	4.4 (2)
C10	0.3737 (4)	0.8808 (3)	0.1604 (3)	3.5 (2)
C11	0.6748 (4)	0.7798 (3)	0.4445 (3)	3.5 (2)
C12	0.5832 (4)	0.7026 (4)	0.5033 (3)	4.1 (2)
C13	0.6481 (5)	0.6770 (4)	0.5826 (3)	4.9 (3)
C14	0.8007 (6)	0.7293 (5)	0.6043 (3)	5.7 (3)
C15	0.8932 (5)	0.8081 (5)	0.5466 (4)	6.0 (3)
C16	0.8313 (4)	0.8321 (4)	0.4661 (3)	4.8 (3)
C17	0.2663 (3)	0.6787 (3)	−0.1588 (2)	2.8 (2)
C18	0.2107 (4)	0.8418 (4)	−0.2164 (3)	4.7 (2)
C19	0.1988 (4)	0.7505 (5)	−0.3285 (3)	5.4 (3)
C20	0.2173 (4)	0.6230 (5)	−0.3566 (3)	5.1 (3)
C21	0.2494 (4)	0.5865 (4)	−0.2725 (3)	3.9 (2)
C22	0.2440 (4)	0.8059 (3)	−0.1318 (3)	3.6 (2)
C23	0.5242 (3)	0.7124 (3)	−0.0390 (2)	2.7 (2)
C24	0.6049 (4)	0.6910 (3)	0.0333 (3)	3.4 (2)
C25	0.7617 (4)	0.7458 (4)	0.0440 (3)	3.9 (2)
C26	0.8412 (4)	0.8221 (4)	−0.0190 (3)	4.1 (2)
C27	0.7634 (4)	0.8446 (4)	−0.0909 (3)	4.1 (2)
C28	0.6064 (4)	0.7904 (3)	−0.1019 (3)	3.6 (2)
H2	0.3628	0.5209	0.1727	3.2
H3	0.0841	0.4461	0.2094	3.2
H4	0.0605	0.6624	0.3827	3.2
H5	0.3405	0.8748	0.4623	3.2
H7	0.0347	0.6166	0.0621	3.2
H8	0.0391	0.8426	0.2458	3.2
H9	0.3275	1.0273	0.3145	3.2
H10	0.4902	0.9282	0.1602	3.2
H12	0.4660	0.6617	0.4906	3.2
H13	0.5618	0.6282	0.6238	3.2
H14	0.8606	0.7156	0.6585	3.2
H15	1.0089	0.8468	0.5654	6.7
H16	0.8976	0.9038	0.4295	3.2
H18	0.1964	0.9391	−0.1906	3.2
H19	0.1738	0.7739	−0.3927	5.8
H20	0.2083	0.5575	−0.4417	5.6
H21	0.2798	0.4999	−0.2864	3.2
H22	0.2575	0.8774	−0.0474	3.2
H24	0.5433	0.6351	0.0819	3.2
H25	0.8076	0.7269	0.1036	3.2
H26	0.9572	0.8593	−0.0096	3.2
H27	0.8197	0.9022	−0.1399	3.2
H28	0.5608	0.8392	−0.1367	3.2

+ 1)$^+$, 100%], 527 [(M + 1)$^+$ - Bu, 70%], 294 [M$^+$ SnBu$_3$, 80%].

Preparation of (Phenylthio)ferrocene (3). To a stirred solution of 5 (3.42 g, 5.86 mmol) in THF (35 mL) at −78 °C was added *n*-BuLi (3.7 mL, 5.92 mmol) dropwise. The red reaction mixture was stirred for an additional 30 min, after which water (50 mL) and diethyl ether (100 mL) were added. The organic layer was separated and washed with brine (2 × 50 mL). After drying over K_2CO_3, the solvent was removed to afford $(C_5H_5)Fe(C_5H_4SPh)$ (3) as a crystalline solid (1.66 g, 5.65 mmol, 96%). Large yellow prisms were obtained upon slow recrystallization from CH_2Cl_2 (1.45 g, 493 mmol, 84%), mp 108–109 °C. ^{1}H NMR ($CDCl_3$): δ 7.19–7.01 (m, 5 H), 4.39 (t, *J* = 1.8 Hz, 2 H), 4.32 (t, *J* = 1.8 Hz, 2 H), 4.25 (s, 5 H). ^{13}C NMR ($CDCl_3$): δ 140.77 (s, ipso Ph), 128.57, 125.81, 124.81 (Ph), 75.63 (ipso Cp), 74.91, 70.11, 69.61 (Cp). MS: *m*/*e* 294 [M$^+$, 100%]. Anal. Calcd for $C_{16}H_{14}FeS$: C, 65.32; H, 4.80. Found: C, 65.57; H, 4.80.

Preparation of 1-(Tri-*n*-butylstannyl)-1′-(diphenylphosphino)ferrocene (6). To a THF (40 mL) solution of 4 (3.53 g, 4.62 mmol) chilled to −78 °C was added *n*-BuLi (2.9 mL, 4.62 mmol). The reaction mixture was stirred for a further 30 min and then treated with PPh_2Cl (1.02 g, 4.62 mmol). The mixture was allowed to warm up to ambient temperature and then stirred for another 2 h. The red reaction mixture was diluted with diethyl ether (100 mL) and washed with water (100 mL) and then brine (2 × 50 mL). The organic layer was dried over K_2CO_3, and the solvents were removed *in vacuo*. The red oil obtained was chromatographed on Al_2O_3 with hexane as eluent to afford $(C_5H_4SnBu_3)Fe(C_5H_4PPh_2)$ as a red oil (2.82 g, 4.28 mmol; 92.6%, lit.[11] yield 93%). ^{1}H NMR ($CDCl_3$): δ 7.41–7.28 (m, 10 H), 4.29 (t, *J* = 1.8 Hz, 2 H), 4.21 (t, *J* = 1.8 Hz, 2 H), 4.03 (q, *J* = 1.8 Hz, 2 H), 3.92 (t, *J* = 1.8 Hz, 2 H), 1.62–1.41 (m, 6 H), 1.40–1.21 (m, 6 H), 1.01–0.93 (m, 6 H), 0.90 (t, *J* = 7 Hz, 9 H). ^{31}P NMR ($CDCl_3$): δ −15.97; lit.[11] δ −11.6 ($CDCl_3$).

Preparation of 1-(Diphenylphosphino)-1′-(phenylthio)ferrocene (7). To a chilled solution of 6 (4.7 g, 7.13 mmol) in

THF (45 mL) at −78 °C was added *n*-BuLi (4.7 mL, 7.52 mmol). The reaction mixture was stirred for another 30 min. PhSSPh (1.6 g, 7.33 mmol) in THF (10 mL) was added dropwise and the reaction mixture stirred overnight at room temperature. The dark-red solution was diluted with ether (100 mL) and washed with degassed water (100 mL) and then brine (2 × 50 mL). The organic layer was dried, and the solvent was removed to give an orange powder. The solid was purified by recrystallization from THF/hexane mixture or by column chromatography on Al_2O_3 with hexane and then THF as eluents (2.9 g, 6.06 mmol, 85%), mp 119–120 °C. ^1H NMR ($CDCl_3$): δ 7.38–6.96 (m, 15 H), 4.45 (t, J = 1.8 Hz, 2 H), 4.29 (t, J = 1.8 Hz, 2 H), 4.21 (t, J = 1.8 Hz, 2 H), 4.18 (q, J = 1.8 Hz, 2 H). ^{13}C NMR ($CDCl_3$): δ 140.44 (s, ipso SPh), 138.67 (d, J = 9.6 Hz, ipso PPh), 133.47 (d, J = 19.4 Hz, PPh), 128.56 (Ph), 128.17 (d, J = 6.8 Hz, PPh), 125.91 (Ph), 124.87 (Ph), 77.21 (ipso Cp), 75.76 (Cp), 74.19 (d, J = 14.3 Hz, CpP), 72.76 (d, J = 3.3 Hz, CpP), 71.62 (CpS). ^{31}P NMR ($CDCl_3$): δ −16.88. MS: *m/e* 478 [M^+, 100%], 401 [$M^+ - Ph$, 15%], 369 [$M^+ - SPh$, 10%]. Anal. Calcd for $C_{28}H_{23}FePS$: C, 70.30; H, 4.85. Found: C, 70.33; H, 4.55.

Preparation of (Phenylthio)diphenylphosphine. Thiophenol (11.02 g, 100 mmol) and sodium metal (2.3 g, 100 mmol) were refluxed in THF (70 mL) for ca. 4 h, during which the solution turned cloudy white. The cloudy white suspension was allowed to settle and the liquid portion removed *via* cannula. The white solid obtained was washed with THF (3 × 50 mL). THF (150 mL) was then added to the white solid to make a fine slurry, which was transferred to another flask (250 mL) *via* cannula leaving some pieces of sodium (0.3 g).

To the cloudy white liquid was added PPh_2Cl[19.2 g, 87 mmol (based on the amount of sodium that reacted)] in THF (10 mL) dropwise over 30 min at −50 °C. The cloudy white solution changed to colorless. The solution was stirred at 25 °C overnight. Water (40 mL) was added, and the organic layer was separated, washed with water (2 × 20 mL), and dried over $MgSO_4$. The solution was filtered and the solvents removed in vacuo to give a colorless oily liquid. The liquid solidified on standing at −4 °C overnight. The solid was recrystallized from hot $CHCl_3$ solution to afford $PhSPPh_2$ (21.5 g, 73 mmol, 84%), mp 49–51 °C (lit.[12] mp 50–52 °C. ^1H NMR ($CDCl_3$): δ 7.80–7.30 (m). ^{31}P NMR ($CDCl_3$): δ 30.3.

Reaction of 1,1′-Dilithioferrocene with (Phenylthio)diphenylphosphine. $PhSPPh_2$ (4.74 g, 16.1 mmol) in benzene (50 mL) was added dropwise to $(C_5H_4Li)_2Fe$ (1) (16.5 mmol) in hexane (20 mL) over 30 min with stirring at −50 °C. The reaction mixture was stirred at room temperature overnight, during which the orange color changed to yellow. Water (50 mL) was added, and the solid that precipitated was filtered off. The solid was washed with water (2 × 20 mL) and then hexane (2 × 20 mL) to give a yellow solid identified by ^1H NMR spectroscopy and to be $(C_5H_4PPh_2)_2Fe$ (3.6 g, 6.5 mmol, 80%, based on $PhSPPh_2$), mp 182–185 °C. Crystals obtained upon slow recrystallization from CH_2Cl_2 melt at 184–185 °C (lit.[13] mp 182–184 °C). ^1H NMR ($CDCl_3$): δ 7.44–7.31 (m, 20 H), 4.21 (t, J = 1.7 Hz, 4 H), 3.95 (t, J = 1.7 Hz, 4 H). ^{31}P NMR ($CDCl_3$): δ −16.5.

X-ray Crystallography. Diffraction measurements were carried out on a Nonius CAD-4 automated diffractometer (Mo Kα radiation) employing the θ–2θ scan method. Unit cells were determined and refined from 25 randomly selected reflections with 2θ in the range 7.94–26.18, 15.80–33.74, 18.86–32.92 and 18.78–34.22° for **8**, **2**, **3**, and **7**, respectively, obtained by using the CAD-4 automatic search, center, index, and least-squares routines. The cell-reduction procedure was performed to ensure no symmetry higher than that of the space groups reported. Intensity data were corrected for Lorentz, polarization, and absorption effects. Data reduction and structure refinements were performed using the NRCC package on a microVAX 3600.[20] The structures were resolved by the heavy-atom method and refined by least-squares recycle routines; all non-hydrogen atom were refined with anisotropic thermal parameters. The atomic scattering curves of Fe, S, P, C, and H were taken from ref 21. The ORTEP drawings of the molecules **8**, **2**, **3**, and **7** are shown in Figures 1–4. Their crystal data summaries are given in Table I. Positional parameters for non-hydrogen atoms are shown in Tables II–V, while the selected bond distances and angles are given in the captions of Figures 1–4 for compounds **8**, **2**, **3**, and **7**, respectively.

Acknowledgment. J.A.A. is grateful to the National Science Council of Taiwan, ROC, for a senior postdoctoral fellowship. We are indebted to the National Science Council for partial financial suport (Grant No. NSC80-0208-M001-04). Thanks are also due to Mr. Y. S. Wen, who collected the diffraction data, to Ms. M. M. Chen, for the ^{31}P NMR spectra and elemental analyses, and to Ms. S. Y. Chang, for mass measurements.

Supplementary Material Available: For the four structures **8**, **2**, **3**, and **7**, listings of crystallographic data summaries, anisotropic thermal parameters, and bond distances and angles (12 pages). Ordering information is given on any current masthead page.

OM910492B

---

(20) Gabe, E. J.; Lee, F. L.; Le Page, Y. In *Crystallographic Computing 3; Data Collection, Structure Determination, Proteins, and Databases*; Sheldrick, G. M., Krueger, C., Goddard, R., Eds.; Clarendon Press: Oxford, England, 1985; p 167–174.

(21) Ibers, J.; Hamilton, W. C., Eds. *International Tables for X-ray Crystallography*; Kynoch Press: Birmingham, England, 1974; Vol. IV, Tables 2.2B and 2.3.1.